Relaxation to Neoclassical Flow Equilibrium

in gyrokinetic theory and gyrofluid computation

B. Scott

Max Planck Institut für Plasmaphysik
Euratom Association
D-85748 Garching, Germany

APS/DPP Conference, Oct 2014

Outline

- **Momentum Conservation in Gyrokinetic Theory**
  — conservation lay and transport equation from field theory

- **Plasma Flow and Electric Field**
  — toroidal momentum is a conserved/transported quantity (like pressure)
  — radial electric field derived as a function of conserved/transported quantities
  — fluid flow picture $\leftrightarrow$ gyrokinetic drifts picture

- **Time Scale Separation and Relaxation**
  — Alfvén, then geodesic, then ion collision, then transport
  — transport and a quasistatic equilibrium
  — simple computational model
  — result in a global gyrofluid computation

Textbook: Tokamak Magnetic Field and MHD Equilibrium

- axisymmetric div-free vector field for the magnetic field

$$\mathbf{B} = I\nabla\varphi + \nabla\psi\times\nabla\varphi$$

- basic flux function is $\psi(R, Z)$
- requirement of MHD equilibrium

$$\mathbf{J}\times\mathbf{B}\cdot\nabla\varphi = 0 \qquad \Longrightarrow \qquad I = I(\psi)$$

Textbook: Tokamak Divergence-free Flows

- axisymmetric div-free vector field for the flow field

$$\mathbf{u} = W R^2 \nabla\varphi + U\mathbf{B} \qquad \mathbf{B}\cdot\nabla U = 0 \qquad \Longrightarrow \qquad U = U(\psi)$$

- toroidal and parallel components

$$u^\varphi \equiv \mathbf{u}\cdot\nabla\varphi = W + U\frac{I}{R^2} \qquad u_\parallel = W\frac{I}{B} + UB$$

- requirement of MHD equilibrium with div-free flow

$$\frac{\partial}{\partial t}\frac{I}{R^2} + \nabla\cdot\frac{I}{R^2}\mathbf{u} = \mathbf{B}\cdot\nabla u^\varphi \qquad \Longrightarrow \qquad W = W(\psi)$$

Textbook: Perpendicular Force Balance

- negligible flow inertia (incl viscosity), allow resistive friction

$$\mathbf{E} = -\frac{\mathbf{u}}{c}\times\mathbf{B} + \frac{1}{nZe}\nabla p + \frac{E_\parallel}{B}\mathbf{B}$$

- assume $\mathbf{E} = -\nabla\phi$, put in the form for $\mathbf{u}$ and dot with $\nabla\psi$ to find

$$\frac{1}{c}WR^2\nabla\varphi\times\mathbf{B}\cdot\nabla\psi = \nabla\psi\cdot\left(\nabla\phi + \frac{1}{nZe}\nabla p\right)$$

- assume ϕ, n, and p are flux functions, pull out $|\nabla\psi|^2$, find

$$\frac{1}{c}W = \frac{\partial\phi}{\partial\psi} + \frac{1}{nZe}\frac{\partial p}{\partial\psi}$$

- this is actually for each ion, so ϕ is set by charge conservation ...

Neoclassical Theory: Poloidal Flow

- the other degree of freedom is poloidal flow
- use orthogonality, $\nabla\varphi \cdot \nabla\theta = 0$ for any reasonable definition of θ
- hence poloidal flow is given solely by U

$$\mathbf{u} \cdot \nabla\theta = U\mathbf{B} \cdot \nabla\theta \qquad\qquad U = \frac{\mathbf{u} \cdot \nabla\theta}{\mathbf{B} \cdot \nabla\theta}$$

- this U is actually the output of several neoclassical codes
  (eg, NEOART, A G Peeters *Phys Plasmas* 7:268 2000)
- again, this is actually for each ion, so ϕ is set by charge conservation ...
  - ◦ the quantity U is set by neoclassical theory (dissipation)
  - ◦ then, the quantity W is set by the toroidal momentum (conservation)

Conserved Toroidal Momentum

- find the *covariant* toroidal component of the flow

$$u_\varphi = R^2 W + UI$$

- with mass density, this is the toroidal angular momentum

$$M_\varphi = \sum_{\text{sp}} nm(R^2 W + UI)$$

- note that "covariant toroidal component" carries the factor of R

Finally, Neoclassical Radial Electric Field

- the inputs are n and p for each species, and M_φ
- then, neoclassical theory gives the quantity U
- then, to fix W therefore $d\phi/d\psi$ ...
- define a radial coordinate $\rho = \rho(\psi)$ as you wish, and $E_r = -d\phi/d\rho$
- solve for W and then plug in its formula, use flux surface average $\langle R^2 \rangle$, find

$$E_r = -\frac{1}{\rho_M \langle R^2 \rangle} \left[\frac{1}{c} \frac{\partial \psi}{\partial \rho} \left(M_\varphi - I \sum_{\text{sp}} nmU \right) - \langle R^2 \rangle \sum_{\text{sp}} \frac{m}{Ze} \frac{\partial p}{\partial \rho} \right]$$

- conventional neoclassical ordering: M_φ is small
  (static force balance: U is small or zero)
- this allows setting the neoclassical E_r with finite-Mach M_φ
- caveat: assumes the determining of U by collisions under finite-Mach M_φ is known

The Gyrokinetic Representation

- based around perp force balance (similar to "reduced fluid"), so we define

$$\nabla_\perp \equiv -\frac{1}{B^2}\mathbf{B}\times(\mathbf{B}\times\nabla) \qquad \nabla_\perp^2 \equiv \nabla\cdot(\nabla_\perp)$$

- the salient small parameter is the ratio ExB vorticity to ion gyrofrequency

$$\Omega_E \equiv \frac{c}{B}\nabla_\perp^2\phi \qquad\qquad \Omega_E/\Omega \sim \delta \ll 1$$

- long-wavelength: ϕ enters the Lagrangian (density $\mathcal{L}$) solely through

$$\phi \qquad \text{or} \qquad u \equiv \frac{1}{2}\left|\nabla_\perp\phi\right|^2 \qquad\qquad v \equiv \nabla_\perp^2\phi$$

- then we define

$$C \equiv -\frac{\partial\mathcal{L}}{\partial\phi} \qquad N \equiv \frac{\partial\mathcal{L}}{\partial u} \qquad P \equiv -\frac{\partial\mathcal{L}}{\partial v}$$

Charge Conservation

- variation of ϕ gives functional derivative $\delta L/\delta\phi$
- result is the polarisation equation

$$C + \nabla \cdot (N \nabla_\perp \phi) + \nabla_\perp^2 P = 0$$

- note that C is charge density of gyrocenters, not particles
- the quantity N gives the polarisability, its whole term is polarisation density
- the quantity P gives the finite gyroradius (FLR) contribution
- charge conservation is the time derivative of this equation
  - define polarisation $\nabla \cdot \mathbf{P} = C$ hence $\mathbf{P} = -\left(N \nabla_\perp \phi + \nabla_\perp P\right)$
- charge conservation is actually $\nabla \cdot \mathbf{J} = 0$ with the polarisation and drift pieces

$$\nabla \cdot \frac{\partial \mathbf{P}}{\partial t} - \frac{\partial C}{\partial t} = 0$$

more on this later, with examples

Momentum Conservation

B Scott, *Phys Plasmas* 17 (2010) 112302

- intimately connected to charge conservation
- conserved toroidal angular momentum includes polarisation and drift pieces

$$M_\varphi \equiv -\frac{1}{c}\left\langle \mathbf{P}\cdot\nabla\psi\right\rangle + I\sum_{\mathrm{sp}}\int d\mathcal{W}\left\langle \frac{fp_z}{B}\right\rangle$$

- toroidal angular momentum conservation is the time derivative of this equation

Toroidal Angular Momentum and Radial Electric Field

- plug in for polarisation using N and P

$$M_\varphi = \frac{1}{c}\left\langle (N\nabla_\perp \phi + \nabla_\perp P)\cdot\nabla\psi \right\rangle + I\sum_{\text{sp}}\int d\mathcal{W}\left\langle \frac{fp_z}{B}\right\rangle$$

- solve for the radial electric field piece

$$-\frac{1}{c}\left\langle N\nabla_\perp\phi\cdot\nabla\psi\right\rangle = \frac{1}{c}\left\langle \nabla_\perp P\cdot\nabla\psi\right\rangle - \left(M_\varphi - I\sum_{\text{sp}}\int d\mathcal{W}\left\langle\frac{fp_z}{B}\right\rangle\right)$$

- iterative approach for general N and P (nonlinear in ϕ)
  - set N and P in terms of zero-Mach limit
  - solve for $d\phi/d\psi$ using $\left\langle N\left|\nabla\psi\right|^2\right\rangle$
  - correct N and P in terms of finite-Mach iterative
  - repeat until converged

Fluid Limit

- as the FLR contributions go to lowest order ...

$$N \to \frac{\rho_M c^2}{B^2} \qquad\qquad P \to \frac{pmc^2}{ZeB^2}$$

- however, we have to link the parallel flow back to the poloidal flow, so use

$$I \sum_{\text{sp}} \int d\mathcal{W} \left\langle \frac{f p_z}{B} \right\rangle = \sum_{\text{sp}} n m u_\parallel \frac{I}{B}$$

and on the fluid side use

$$u_\parallel \frac{I}{B} = W \frac{I^2}{B^2} + UI \qquad\qquad M_\varphi = \sum_{\text{sp}} nm(R^2 W + UI)$$

hence

$$\sum_{\text{sp}} n m u_\parallel \frac{I}{B} = \frac{I^2}{R^2 B^2} \left(M_\varphi + \sum_{\text{sp}} nmU \frac{|\nabla\psi|^2}{I} \right)$$

- the geometry pieces combine such that

$$M_\varphi - I\sum_{\text{sp}}\int d\mathcal{W}\left\langle\frac{fp_z}{B}\right\rangle \approx \left\langle\frac{|\nabla\psi|^2}{R^2B^2}\right\rangle\left(M_\varphi - \sum_{\text{sp}} nmUI\right)$$

hence the radial electric field equation is

$$-\frac{1}{c}\left\langle N\nabla_\perp\phi\cdot\nabla\psi\right\rangle = \frac{1}{c}\left\langle\nabla_\perp P\cdot\nabla\psi\right\rangle - \left\langle\frac{|\nabla\psi|^2}{R^2B^2}\right\rangle\left(M_\varphi - \sum_{\text{sp}} nmUI\right)$$

which becomes in the fluid limit

$$-\rho_M\left\langle R^2\right\rangle\frac{\partial\phi}{\partial\psi} = \left\langle R^2\right\rangle\sum_{\text{sp}}\frac{m}{Ze}\frac{\partial p}{\partial\psi} - \frac{1}{c}\left(M_\varphi - \sum_{\text{sp}} nmUI\right)$$

- and this corresponds to what we had before

$$E_r = -\frac{1}{\rho_M\left\langle R^2\right\rangle}\left[\frac{1}{c}\frac{\partial\psi}{\partial\rho}\left(M_\varphi - I\sum_{\text{sp}} nmU\right) - \left\langle R^2\right\rangle\sum_{\text{sp}}\frac{m}{Ze}\frac{\partial p}{\partial\rho}\right]$$

Bottom Line

- gyrokinetic field theory gives a description of the conserved momentum
- the electric field is given in terms of conserved quantities
  and the neoclassical poloidal rotation
- in the fluid limit the gyrokinetic description recovers the fluid expression
- as ever:

> the caveat is the ability of the collisional model
> to give the neoclassical poloidal rotation (U)

- if a gyrokinetic model can do this it can capture neoclassical flow
  - ◦ strict neoclassical ordering of small M_φ is not needed in either case
  - ◦ neoclassical ordering of linear ϕ and $\nabla\phi$ is not needed in the gyrokinetic case

example: where do higher order terms go?

- our finite-Mach gyrokinetic Lagrangian (Miyato et al, *JPSJ* 78:104501 2009)

$$L = \cdots - \sum_{\text{sp}} \int d\Lambda\, f \left(e\phi + e\frac{\rho_L^2 + \rho_E^2}{4}\nabla_\perp^2 \phi - nm\frac{u_E^2}{2} \right)$$

where

$$\mathbf{u}_E = \frac{c}{B^2}\mathbf{B}\times\nabla\phi \qquad \rho_E^2 = \frac{u_E^2}{\Omega^2} \qquad \rho_L^2 = \frac{2\mu B}{\Omega^2}$$

- find polarisation quantities

$$C = \sum_{\text{sp}} ne \qquad N = \sum_{\text{sp}} \frac{nmc^2}{B^2}\left(1 - \frac{\Omega_E}{2\Omega}\right) \qquad P = \sum_{\text{sp}} \frac{mc^2}{2eB^2}\left(p_\perp + nm\frac{u_E^2}{2}\right)$$

where the moment variables are given by

$$n = \int d\mathcal{W}\, f \qquad nmu_\parallel = \int d\mathcal{W}\, p_z\, f \qquad p_\perp = \int d\mathcal{W}\, \mu B\, f$$

- now find polarisation contribution to momentum

$$-\frac{1}{c}\mathbf{P}\cdot\nabla\psi = \frac{1}{c}\left|\nabla\psi\right|^2\left(N\frac{\partial\phi}{\partial\psi}+\frac{\partial P}{\partial\psi}\right)$$

$$-\frac{1}{c}\mathbf{P}\cdot\nabla\psi = \frac{1}{c}\left|\nabla\psi\right|^2\left(\frac{\rho_M c^2}{B^2}\frac{\partial\phi}{\partial\psi}+\frac{\partial P}{\partial\psi}-\frac{\rho_M c^2}{B^2}\frac{\Omega_E}{2\Omega}\frac{\partial\phi}{\partial\psi}\right)$$

- put into the iteration scheme for the radial electric field

$$-\frac{1}{c}\left\langle N_0\left|\nabla\psi\right|^2\right\rangle\frac{\partial\phi}{\partial\psi} = \frac{1}{c}\left\langle\left|\nabla\psi\right|^2\left(N_1\frac{\partial\phi}{\partial\psi}+\frac{\partial P}{\partial\psi}\right)\right\rangle - \left\langle\frac{\left|\nabla\psi\right|^2}{R^2B^2}\right\rangle\left(M_\varphi-\sum_{\mathrm{sp}}nmUI\right)$$

  where for these purposes we regard the coefficient nmU as a flux function and denote N_0 and N_1 as

$$N_0 = \frac{\rho_M c^2}{B^2} \qquad\qquad N_1 = -N_0\frac{\Omega_E}{2\Omega}$$

- higher order terms are in N_1 and P and are small by δ for equilibrium flows

Relaxation to Equilibrium from Arbitrary Initial State

- time scale separation

$$\omega_A = \frac{v_A}{qR} \quad \gg \quad \omega_S = \frac{c_s}{qR} \quad \gg \quad \omega_C = (\nu_i)_{NC} \quad \gg \quad \omega_T = \tau_E^{-1}$$

- various pieces relaxing on these scales:
  - current and vorticity sidebands on ω_A
  - flow, density/pressure, ion thermal sidebands on ω_S
  - bootstrap current, neoclassical poloidal ion flow on ω_C
  - transport of conserved quantities on ω_T

- definition of a sideband (Alfvén pieces, ϖ is ion vorticity)

$$\left\langle J_\parallel \cos\theta \right\rangle \qquad \left\langle \varpi \sin\theta \right\rangle \qquad \text{driven by} \quad \frac{\partial}{\partial \rho} \left\langle p \right\rangle$$

relaxation in a fluid model

- we can't do this with a 4-field model because we need ion temperature T_i
  - hence for consistency keep also T_e and heat fluxes $q_{e\parallel}$ and $q_{i\parallel}$
- first use of these equations (e.g., always use a dynamical heat flux)
  PPCF 40 (1998) 823 and *Contrib Plasma Phys* 38 (1998) 171
- equations shown in normalised fluxtube form, see *Phys Plasmas* 12 (2005) 102307
- for correspondence fluid to gyrofluid, see *Phys Plasmas* 14 (2007) 102318
- for correspondence gyrofluid to gyrokinetic, see *Phys Plasmas* 17 (2010) 102306
- coupling parameters: $\omega_B = 2\delta L_\perp/R$ and $b^s = L_\perp/qR$ with $\delta = \rho_s/L_\perp$
- for a global model use $L_\perp \to a$ and keep $1/\rho$ effects

- neglecting nonlinearities, FLR/anisotropy effects, basic model without dissipation is

$$\frac{\partial \varpi}{\partial t} = B\nabla_{\parallel}\frac{J_{\parallel}}{B} - \mathcal{K}\left(p_e + p_i\right) \qquad \varpi = \nabla_{\perp}^2\left(\phi + p_i\right)$$

$$\frac{\partial}{\partial t}\left(\beta_e A_{\parallel} + \mu_e J_{\parallel}\right) = -\nabla_{\parallel}\left(\phi - p_e\right) \qquad J_{\parallel} = -\nabla_{\perp}^2 A_{\parallel}$$

$$\frac{\partial n}{\partial t} = B\nabla_{\parallel}\frac{J_{\parallel} - u_{\parallel}}{B} - \mathcal{K}\left(p_e - \phi\right)$$

$$\mu_i \frac{\partial u_{\parallel}}{\partial t} = -\nabla_{\parallel}\left(p_e + p_i\right)$$

$$\frac{3}{2}\frac{\partial T_e}{\partial t} = B\nabla_{\parallel}\frac{J_{\parallel} - u_{\parallel} - q_{e\parallel}}{B} - \mathcal{K}\left(p_e - \phi + \frac{5}{2}T_e\right)$$

$$\mu_e \frac{\partial q_{e\parallel}}{\partial t} = -\frac{5}{2}\nabla_{\parallel} T_e$$

$$\frac{3}{2}\frac{\partial T_i}{\partial t} = B\nabla_{\parallel}\frac{J_{\parallel} - u_{\parallel} - q_{i\parallel}}{B} - \mathcal{K}\left(p_e - \phi - \frac{5}{2}\tau_i T_i\right)$$

$$\mu_i \frac{\partial q_{i\parallel}}{\partial t} = -\frac{5}{2}\tau_i \nabla_{\parallel} T_i$$

free energy theorem

- conserved free energy density

$$\mathcal{E} = \frac{1}{2}\Bigg[\left|\delta\nabla_\perp\left(\phi + p_i\right)\right|^2 + (1+\tau_i)n^2 + \frac{3}{2}T_e^2 + \frac{3}{2}\tau_i T_i^2 \\ + \beta_e\left|\delta\nabla_\perp A_\parallel\right|^2 + \mu_e J_\parallel^2 + \mu_i u_\parallel^2 + \frac{2}{5}\mu_e {q_e}_\parallel^2 + \frac{2}{5}\mu_i {q_i}_\parallel^2 \Bigg]$$

- spatially averaged integral

$$\frac{\partial}{\partial t}\int d\mathcal{V}\,\mathcal{E} = 0 \qquad\qquad d\mathcal{V} = \frac{1}{\pi}\rho\,d\rho\,d\theta$$

- proof: multiply equations respectively by

$$-\left(\phi + p_i\right) \qquad J_\parallel \qquad (1+\tau_i)n \qquad u_\parallel \qquad T_e \qquad \frac{2}{5}q_{e\parallel} \qquad \tau_i T_i \qquad \frac{2}{5}q_{i\parallel}$$

  add them, and integrate over domain

Braginskii dissipation model

- parallel dissipation only, thermal forces in electrons only
- resistivity and thermal force in Ohm's law and electron heat flux
  - thermal conduction only in ion heat flux (see *PPCF* 39 (1997) 1635)

$$E_\parallel = \cdots + \mu_e \nu_e \left[0.51 J_\parallel + \frac{0.71}{3.2} \left(q_{e\parallel} + 0.71 J_\parallel \right) \right]$$

$$\mu_e \frac{\partial q_{e\parallel}}{\partial t} = \cdots - \mu_e \nu_e \frac{5/2}{3.2} \left(q_{e\parallel} + 0.71 J_\parallel \right)$$

$$\mu_i \frac{\partial q_{i\parallel}}{\partial t} = \cdots - \mu_i \nu_i \frac{5/2}{3.9} q_{i\parallel}$$

- electron and ion energetics

$$\frac{2}{5} \mu_e q_{e\parallel} \frac{\partial q_{e\parallel}}{\partial t} - E_\parallel J_\parallel = \cdots - \mu_e \nu_e \left[0.51 \left(J_\parallel \right)^2 + \frac{1}{3.2} \left(q_{e\parallel} + 0.71 J_\parallel \right)^2 \right]$$

$$\frac{2}{5} \mu_i q_{i\parallel} \frac{\partial q_{i\parallel}}{\partial t} = \cdots - \mu_i \nu_i \frac{1}{3.9} \left(q_{i\parallel} \right)^2$$

- note: positive-definite damping, the basis for all subsequent dissipation models

Landau closure model

- expect: no dissipation of equilibrium, thermodynamically consistent damping
- solution: dissipation acts on total heat flux divergence,
  under conditions of energetic consistency
- total heat flux divergence (parallel, diamagnetic), each species

$$D \equiv B\nabla_{\parallel}\frac{q_{\parallel}}{B} - \mathcal{K}\left(\frac{5}{2}\tau T\right)$$

- involves both T and $q_{\parallel}$, must be in both their equations (use $VL = \sqrt{\tau/\mu}\, qR$)

$$\frac{3}{2}\frac{\partial T}{\partial t} = \cdots - \mathcal{K}\left(\mu VLD\right) \qquad\qquad \mu\frac{\partial q_{\parallel}}{\partial t} = \cdots + \nabla_{\parallel}\mu VLD$$

- signed charge ratios: $\mu = m/ZM_D$ and $\tau = T/ZT_e$, energetics with $a = nZ/n_e$
  - ◦ obtain positive-definite damping $\implies$ thermodynamically correct
  - ◦ no damping after $D \to 0$

$$a\left(\frac{3}{2}\tau T\frac{\partial T}{\partial t} + \frac{2}{5}\mu q\frac{\partial q}{\partial t}\right) = \cdots - \frac{2}{5}a\mu VLD^2$$

neoclassical viscosity model

- start: thermal force effect in parallel flow equation
- hence: corresponding thermal flux terms in ion parallel heat-flux equation
- final: additional diagonal term in the latter $\implies$ neoclassical transport
- in parallel flow and ion heat flux equations

$$\mu_i \frac{\partial u_\parallel}{\partial t} = \cdots + B\nabla_\parallel \frac{\nu_{NC}}{B} \nabla_\parallel \left(u_\parallel + \alpha_{NC} q_{i\parallel} \right)$$

$$\mu_i \frac{\partial q_{i\parallel}}{\partial t} = \cdots + B\nabla_\parallel \frac{5}{2} \frac{\nu_{NC}}{B} \nabla_\parallel \left[\chi_{NC} q_{i\parallel} + \alpha_{NC} \left(u_\parallel + \alpha_{NC} q_{i\parallel} \right) \right]$$

- energetics (ions have $a = 1$ and $\mu = 1$):

$$\mu_i \left(u_\parallel \frac{\partial u_\parallel}{\partial t} + \frac{2}{5} q_{i\parallel} \frac{\partial q_{i\parallel}}{\partial t} \right) = \cdots - \nu_{NC} \left(u_\parallel + \alpha_{NC} q_{i\parallel} \right)^2 - \nu_{NC} \chi_{NC} \left(q_{i\parallel} \right)^2$$

- first term does flow equilibrium, no dissipation in dissipative equilibrium
- only the χ_{NC} term does actual neoclassical transport

basic sideband assumption of quasistatically evolving equilibrium

B Scott, *New J Phys* 7 (2005) 92

- flux surface average in vorticity and current sideband equations

$$\frac{\partial}{\partial t}\left\langle \varpi \sin\theta \right\rangle = -b^s \left\langle J_\parallel \cos\theta \right\rangle - \frac{\omega_B}{2}\frac{\partial}{\partial x}\left\langle p_e + p_i \right\rangle$$

$$\frac{\partial}{\partial t}\left\langle \left(\beta_e A_\parallel + \mu_e J_\parallel\right)\cos\theta \right\rangle = -b^s \left\langle (\phi - p_e)\sin\theta \right\rangle - \eta \left\langle J_\parallel \cos\theta \right\rangle$$

- time scale of these is ω_A, so for $\omega \ll \omega_A$ the $\partial/\partial t$ term is small/neglected
  - resulting balances can be combined in derivations, eg,

$$\omega_B \frac{\partial}{\partial x}\left\langle (\phi - p_e)\sin\theta \right\rangle = \frac{\eta}{2}\frac{{\omega_B}^2}{b^{s\,2}}\frac{\partial^2}{\partial x^2}\left\langle p_e + p_i \right\rangle$$

- however, if the right hand sides are out of balance, then the reaction occurs at $\omega \sim \omega_A$

- hence the time derivative should not be *a priori* ordered in a multi-scale process
  - except for $\omega \ll (k_\perp v_A, \Omega)$ as required by the gyrokinetic description

force balance in quasistatically evolving equilibrium

- do the same for the zonal vorticity equation ($B\nabla_\parallel$ is annihilated)

$$\frac{\partial}{\partial t}\left\langle \varpi \right\rangle = -\omega_B \frac{\partial}{\partial x}\left\langle (p_e + p_i)\sin\theta \right\rangle$$

- follow the coupling chain, assume ω_A scales are in balance (keep τ_i factors)
  - here neglect collisional effects since $\omega_S \ll \omega_C$

$$\frac{3}{2}\frac{\partial}{\partial t}\left\langle (p_e + p_i)\sin\theta \right\rangle = \frac{5}{2}\left(1+\tau_i\right) D_s + D_i$$

$$\mu_i \frac{\partial}{\partial t}\left\langle u_\parallel \cos\theta \right\rangle = -b^s \left\langle (p_e + p_i)\sin\theta \right\rangle$$

$$\mu_i \frac{\partial}{\partial t}\left\langle q_{i\parallel} \cos\theta \right\rangle = -\frac{5}{2}\tau_i b^s \left\langle T_i \sin\theta \right\rangle - a_{Li}\left(D_i\right)$$

where the sideband flow and ion heat flux gyrocenter divergences are given by

$$D_s = b^s \left\langle u_\parallel \cos\theta \right\rangle + \frac{\omega_B}{2}\frac{\partial}{\partial x}\left\langle \phi + p_i \right\rangle$$

$$D_i = b^s \left\langle q_{i\parallel} \cos\theta \right\rangle + \frac{\omega_B}{2}\frac{\partial}{\partial x}\left\langle \frac{5}{2}\tau_i T_i \right\rangle$$

character of the almost collisionless equilibrium

- system does not evolve if there is no pressure/thermal or divergence sideband
- condition of balance is therefore that these vanish
  - when divergences balance the divergence-dissipation closure ceases effect as well
- putting these in, the zonal variables do not evolve on $\omega \ll \omega_C$ (neglect also η)

$$\frac{\partial}{\partial t}\langle \varpi \rangle = -\omega_B \frac{\partial}{\partial x}\langle (p_e + p_i)\sin\theta \rangle = 0$$

$$\frac{\partial}{\partial t}\langle n \rangle = \omega_B \frac{\partial}{\partial x}\langle (\phi - p_e)\sin\theta \rangle = 0$$

$$\frac{3}{2}\frac{\partial}{\partial t}\langle T_e \rangle = \omega_B \frac{\partial}{\partial x}\left\langle \left(\phi - p_e - \frac{5}{2}T_e\right)\sin\theta \right\rangle = 0$$

$$\frac{3}{2}\frac{\partial}{\partial t}\langle T_i \rangle = \omega_B \frac{\partial}{\partial x}\left\langle \left(\phi - p_e + \frac{5}{2}\tau_i T_i\right)\sin\theta \right\rangle = 0$$

collisional viscosity in quasistatically evolving equilibrium

- now, for $\omega \sim \omega_C$ we put the collisions back in
  - but in doing this assume Alfvén and geodesic/acoustic balances

- the main statement is that the divergences remain close to zero

- recall the flow equation

$$\mu_i \frac{\partial u_\parallel}{\partial t} = -\nabla_\parallel \left(p_e + p_i\right) + B\nabla_\parallel \frac{\nu_{NC}}{B} \nabla_\parallel \left(u_\parallel + \alpha_{NC} q_{i\parallel}\right)$$

- the flow sideband equation in electron/ion balance becomes

$$\left\langle \left(p_e + p_i\right) \sin\theta \right\rangle = -\nu_{NC} b^s \left\langle \left(u_\parallel + \alpha_{NC} q_{i\parallel}\right) \cos\theta \right\rangle$$

- with divergence balance this goes into the vorticity equation as

$$\frac{\partial}{\partial t} \left\langle \varpi \right\rangle = -\nu_{NC} \frac{{\omega_B}^2}{2} \frac{\partial^2}{\partial x^2} \left\langle \phi + p_i + \frac{5}{2} \alpha_{NC} T_i \right\rangle$$

evolution of the quasistatic equilibrium on transport time scales

- the main point is that for $\omega \sim \omega_C$ we have

$$\frac{\partial}{\partial t}\left\langle \varpi \right\rangle = -\nu_{NC}\frac{{\omega_B}^2}{2}\frac{\partial^2}{\partial x^2}\left\langle \phi + p_i + \frac{5}{2}\alpha_{NC}T_i \right\rangle$$

- hence for $\omega \sim \omega_T \ll \omega_C$ we have (regularity at the axis)

$$\frac{\partial}{\partial x}\left\langle \phi + p_i + \frac{5}{2}\alpha_{NC}T_i \right\rangle = 0$$

- this is nothing more/less than the statement of the neoclassical electric field
  - ◦ it is pinned on collisional time scales
  - ◦ behind that, the geodesic/acoustic clamp holds ion force/divergence balance
  - ◦ behind that, the Alfvén/electron clamp holds electron force/divergence balance

- hence for $\omega \sim \omega_T$ the $\partial/\partial t$ is small everywhere

except for (zonal components of) conserved quantities

2-D Axisymmetric Computational Model

- 2-D global model: 129 points $0 < \rho < 1$ and ± 8 Fourier modes ($\theta \leftrightarrow l$)
  - use l'Hopital's rule at the magnetic axis for $1/\rho$ terms
- keep radial profiles and higher sidebands ($l > 1$)
  - continuum damping is how the Alfvén part relaxes
  - cleaner sideband cascade prevents $l = 1$ pile-up
- Karniadakis time step allows long-time integration
- **no ordering on partial time derivative**
- set parameters and q-profile for mid-size tokamak core

$$a/\rho_s = 200 \qquad q = 1.5 + 2.5\rho^2 \qquad R/a = 3.3 \qquad \beta_e = 2 \times 10^{-3}$$

- species parameters:

$$\mu_e = 2.72 \times 10^{-4} \qquad \mu_i = 1 \qquad \tau_i = 1$$

- constants and correct collisional damping rates: $\alpha_{NC} = -0.6 \quad \chi_{NC} = 1.5$

$$\nu_e a/c_s = 10^{-1} \qquad \nu_i/\nu_e = \sqrt{\mu_e/2} \qquad \nu_{NC} = 10^{-2}\, V_i/qR$$

initial evolution on Alfvén time scale

- initial state, zonal profiles, all other quantities zero

$$\varpi = 0 \qquad n = 0.7(1 + \cos \pi\rho) \qquad T_e = T_i = 2.0(1 + \cos \pi\rho)$$

- evolution shown to $20\, a/c_s$
- Alfvén responses follow v_A/qR which has shear
- outward propagation for strong shear
  - ever-narrowing layers

evolution on geodesic scale

- evolution shown to $200\, a/c_s$
- still some finite Alfvén ringing especially at edge
- geodesic response most apparent in ion heat channel and zonal ϕ
- radial electric field goes into collisionless force balance
- MHD equilbirium almost formed

evolution on neoclassical collisional scale

- evolution shown to $2000\, a/c_s$
- Alfvén and geodesic ringing is gone
- MHD equilbirium well formed
- flow equilbirium is also very solid
- hence force balance very strict (see energetics)
- radial electric field and flow pattern slowly relaxes (see energetics and profiles)

evolution on neoclassical transport scale

- evolution shown to $20000\, a/c_s$
- MHD and flow equilbiria very strict (see energetics)
- all relaxation due to collisions with other parts in equilibrium
- case with $\chi_{NC} = 0$ shows no transport
  - demonstrates the difference between equilibrium clamping and transport

long-term evolution

- evolution shown to 200000 a/c_s
- transport stops when ion temperature gradient is gone
- equilibrium force balance with just density and electron temperature gradients
  - these slowly relax due to electron collisionality (much weaker)
- **there are no issues about how long this can be run**
- to be able to say that ...
  - you need exact energetic consistency in the collisionless part of the model
  - you also need thermodynamically correct dissipation

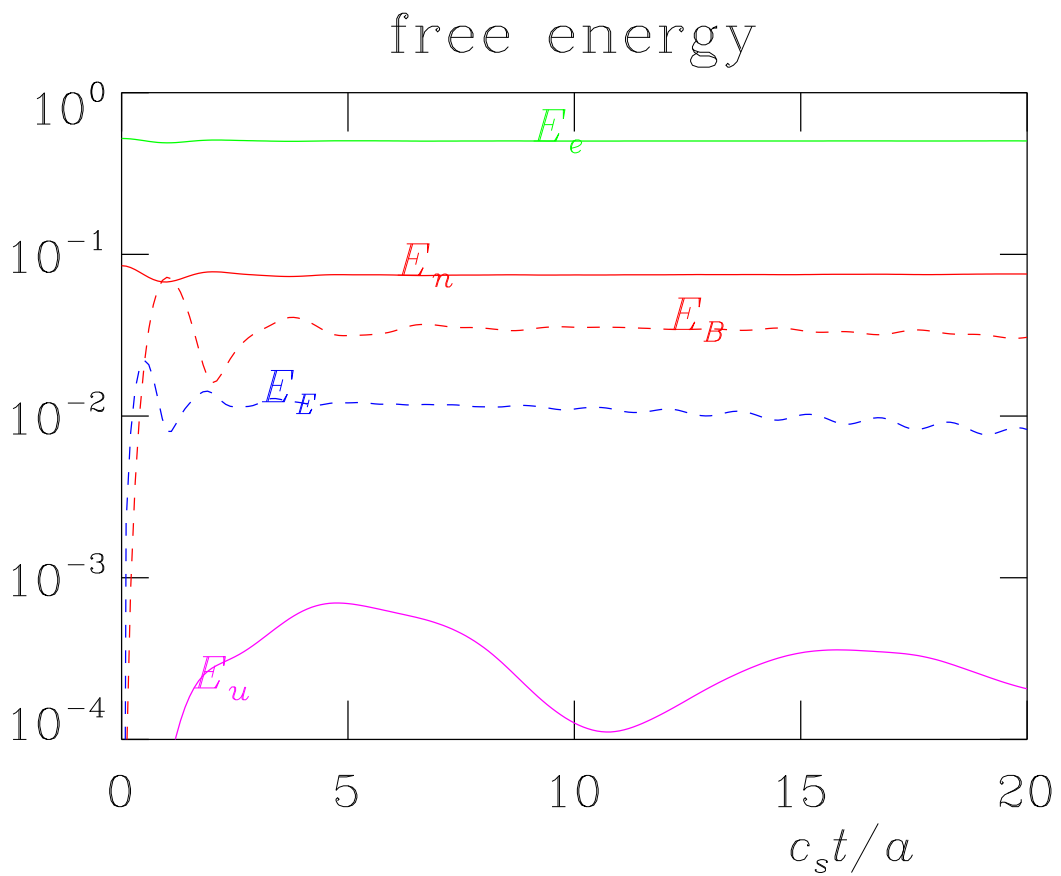

Fig. 1. Time traces of free energy components (due to ExB and diamagnetic ion flow 'E', density 'n', electron temperature 'e', magnetic field and parallel electron flow 'B', and parallel ion flow 'u'), showing the initial Alfvén response for $t < 5$ and in E_u the initial acoustic response. The Alfvén oscillations do not die out so fast, however, as shown in the next few figures. The ion temperature free energy E_i, not shown, is very close to E_e.

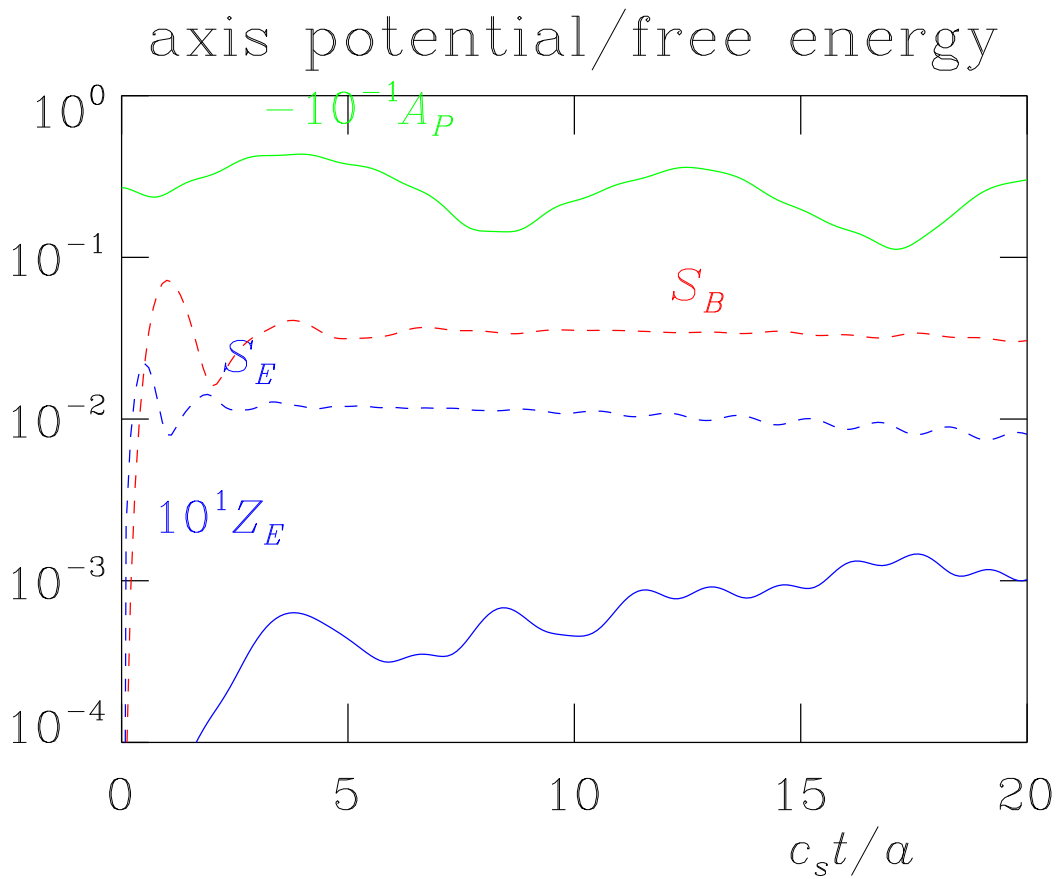

Fig. 2. Time traces of $10^{-1}\times$ the axis value of ϕ (A_P), $10\times$ the zonal component of the ion ExB/diamagnetic flow energy (Z_E), and the $l = 1$ sideband components of ion ExB/diamagnetic flow (S_E) and magnetic field/parallel electron flow (S_B) energies. Comparison to Fig. 1 shows that S_E and S_B nearly cover the total values E_E and E_B, also shown by the small level of Z_E. Of these signals, only A_P reflects the underlying acoustic oscillation which is otherwise swamped by the Alfvén responses.

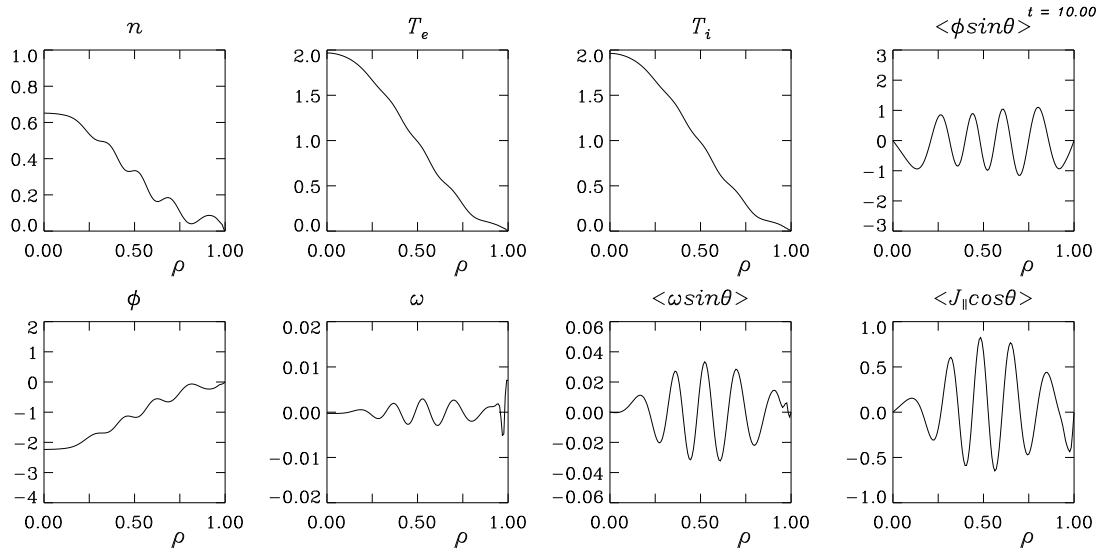

Fig. 3. Profiles (functions of ρ independent of θ) of the state at $t = 10a/c_s$ showing zonal components of the density n, both temperatures $T_{e,i}$, the electrostatic potential ϕ and the vorticity ϖ, the $\sin\theta$ sidebands of ϕ and ϖ, and the $\cos\theta$ sideband of the parallel current $J_{||}$. The Alfvén oscillation layers are seen in the three sidebands; animation of this figure from $t = 0$ to 20 in steps of 0.1 show growth, decay, and slow damping of the sizes as the layers move outward and narrow in width. Oscillation layers can also be seen in n, ϕ and ϖ and to a lesser extent discerned in $T_{e,i}$. The zonal ϕ is in the vicinity of but not exactly at the statis force-balance level, since at the same time the acoustic oscillations are in progress.

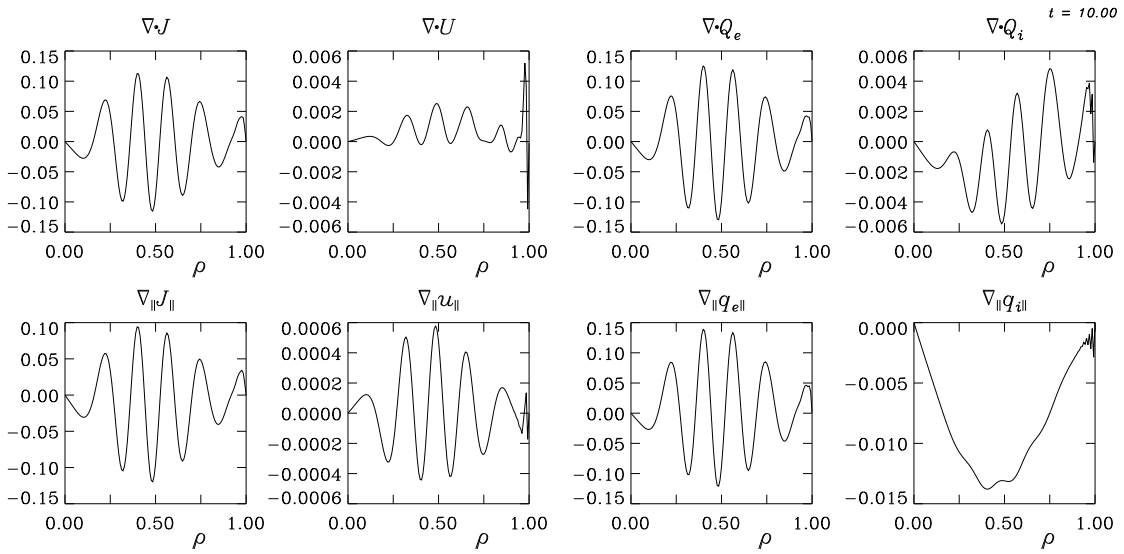

Fig. 4. Profiles (functions of ρ independent of θ) at $t = 10a/c_s$ of the $\sin\theta$ component of the total gyrocenter divergences (that is, minus the polarisation component) in the current $\mathbf{J}$, ion flow $\mathbf{U}$, and electron and ion heat fluxes $\mathbf{Q}_{e,i}$, together with their corresponding parallel divergences $\nabla_\parallel$ on $J_\parallel$, $u_\parallel$, $q_{e\parallel}$, and $q_{i\parallel}$, respectively (note $\nabla_\parallel J_\parallel$ is actually $B\nabla_\parallel(J_\parallel/B)$, etc, but in this model $B = B_0$). In each case a total divergence consists of a geodesic curvature part acting on the zonal component of a state variable (plus the much smaller $l = 2$ sideband) and a parallel part acting on the $\cos\theta$ sideband of the coresponding flux variable, with the associated pairs being those given in Eqs. (70-73). The top row gives the total and the bottom row the parallel part. The ratio top/bottom row gives the closeness of equilibration. For $t = 10$ the perturbations due to the propagating Alfvén oscillation layers are very strong.

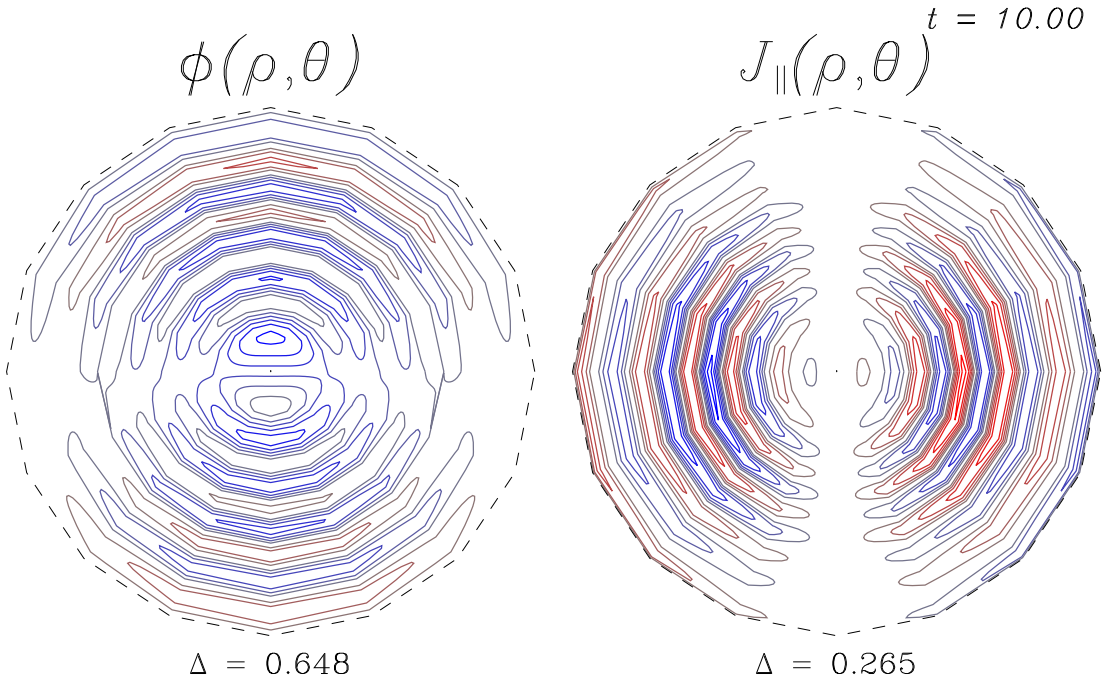

Fig. 5. Snapshot of the state at $t = 10a/c_s$ showing the electrostatic potential ϕ and the parallel current $J_{\|}$. In each case red/blue are positive/negative and Δ gives the interval in normalised units. The system has not yet relaxed into force-balance equilibrium, as the narrow radial layers in the sideband quantities are the dominant component of both variables. Animation of this figure from $t = 0$ to 20 in steps of 0.1 shows that for about $t > 5$ the amplitude of the layers is only weakly oscillatory while the layers drift spatially outward towards the boundary.

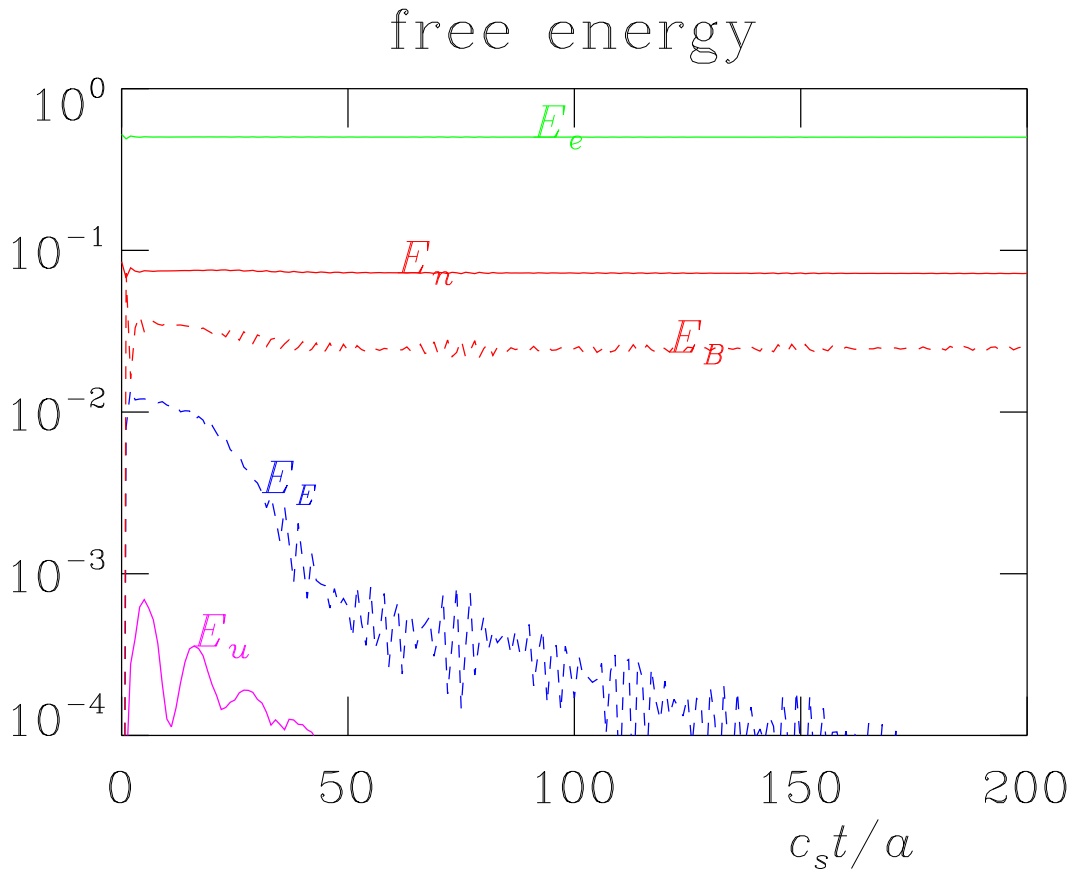

Fig. 6. Time traces of free energy components (due to ExB and diamagnetic ion flow 'E', density 'n', electron temperature 'e', magnetic field and parallel electron flow 'B', and parallel ion flow 'u'). Comparison to Fig. 1 shows that the ion flow channels E_E and E_u have dropped away while the magnetic/electron parallel flow energy E_B finds balance against the thermal free energy channels (E_i, not shown, is very close to E_e). This reflects the energy in the Pfirsch-Schlüter current and its associated magnetic field perturbation (the Shafranov shift).

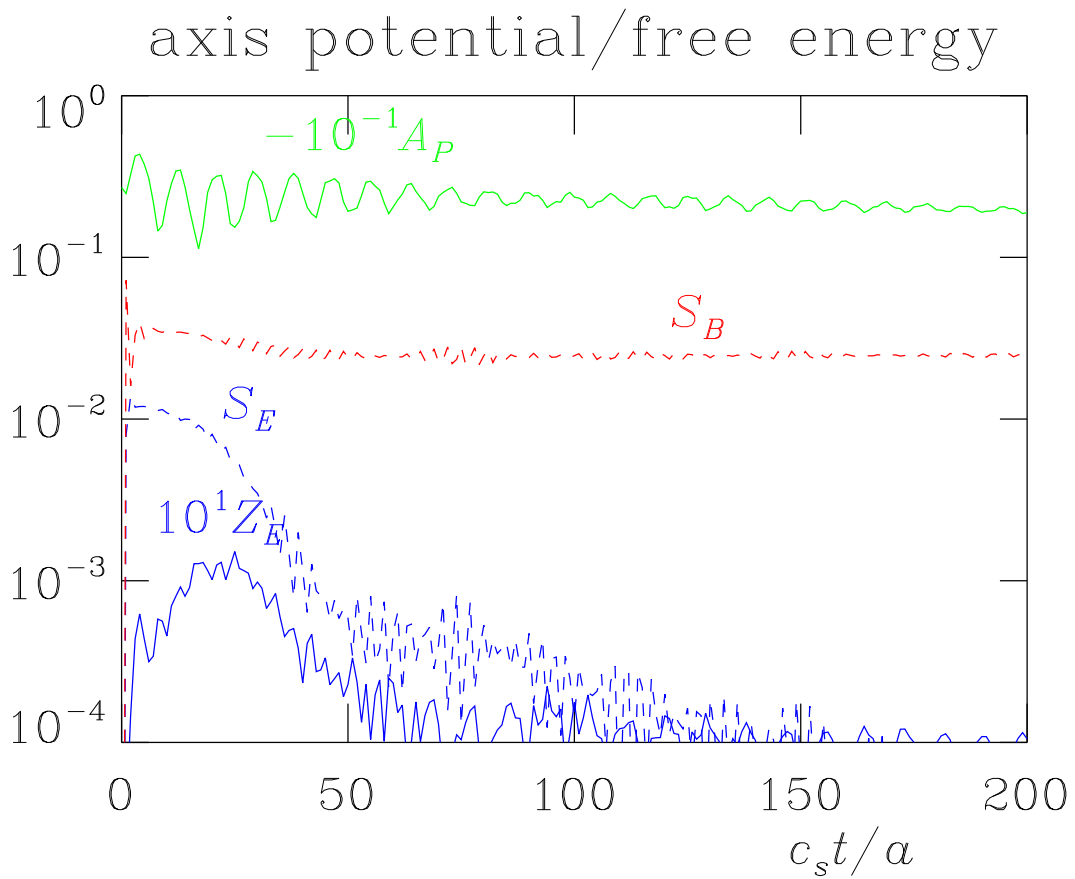

Fig. 7. Time traces of $10^{-1}\times$ the axis value of ϕ (A_P), $10\times$ the zonal component of the ion ExB/diamagnetic flow energy (Z_E), and the $l = 1$ sideband components of ion ExB/diamagnetic flow (S_E) and magnetic field/parallel electron flow (S_B) energies. Comparison to Fig. 6 shows that almost all of E_E and E_B are in their respective sidebands S_E and S_B with Z_E much smaller. The geodesic oscillations are visible in A_P and these are mostly damped for $t > 100$. Comparison to Fig. 2 shows the drop in the ion flow energy while the amplitude A_P and the magnetic field/parallel electron flow energy find equilibration at finite levels.

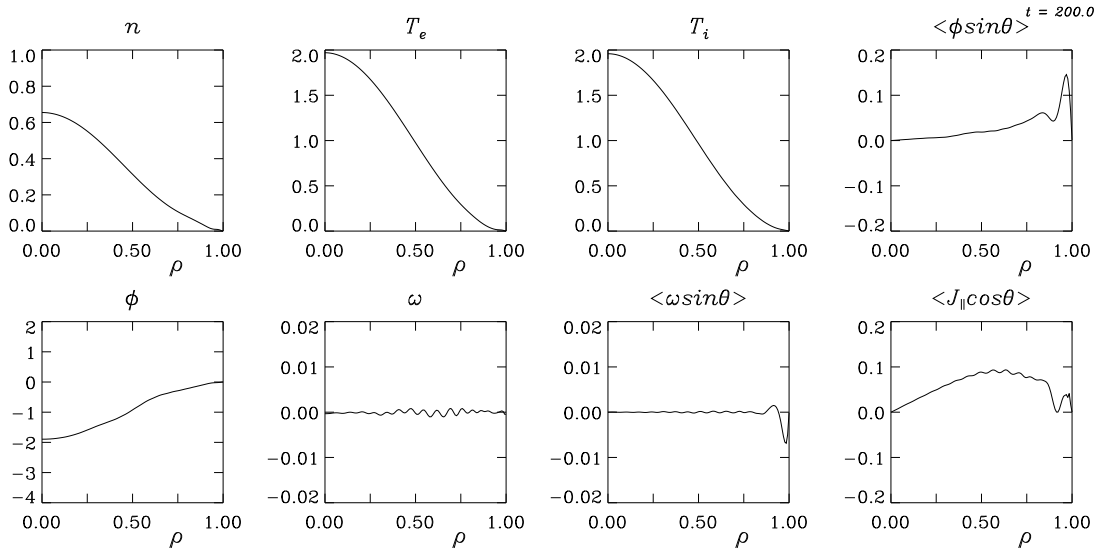

Fig. 8. Profiles (functions of ρ independent of θ) of the state at $t = 200a/c_s$ showing zonal components of the density n, both temperatures $T_{e,i}$, the electrostatic potential ϕ and the vorticity ϖ, the $\sin\theta$ sidebands of ϕ and ϖ, and the $\cos\theta$ sideband of the parallel current $J_{||}$. Comparison to Fig. 3, against which the change in scale for the sideband quantities is to be noted, shows that the Alfvén oscillation layers in the three sidebands have mostly damped away except for some persistence at the outer boundary (driven by the ϖ and $J_{||}$ sidebands, with ϕ the response felt further inward), and except for this the system is close to force-balance equilibration.

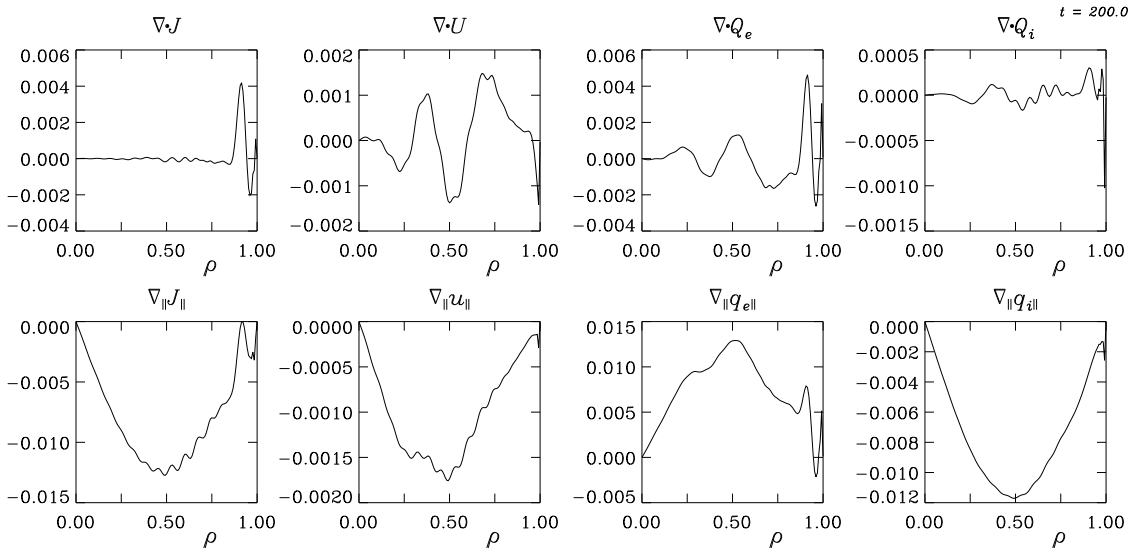

Fig. 9. Profiles (functions of ρ independent of θ) at $t = 200a/c_s$ of the $\sin\theta$ component of the total gyrocenter divergences (that is, minus the polarisation component) in the current $\mathbf{J}$, ion flow $\mathbf{U}$, and electron and ion heat fluxes $\mathbf{Q}_{e,i}$, together with their corresponding parallel divergences $\nabla_\parallel$ on $J_\parallel$, $u_\parallel$, $q_{e\parallel}$, and $q_{i\parallel}$, respectively (note $\nabla_\parallel J_\parallel$ is actually $B\nabla_\parallel(J_\parallel/B)$, etc, but in this model $B = B_0$). In each case a total divergence consists of a geodesic curvature part acting on the zonal component of a state variable (plus the much smaller $l = 2$ sideband) and a parallel part acting on the $\cos\theta$ sideband of the coresponding flux variable, with the associated pairs being those given in Eqs. (70-73). The top row gives the total and the bottom row the parallel part. The ratio top/bottom row gives the closeness of equilibration. For $t = 200$ the Alfvén oscillations reflect nearly complete relaxation while the other components remain out of balance. Animation of this figure in the range $100 < t < 1000$ show outwardly propagating geodesic oscillations in the top row $\nabla \cdot \mathbf{U}$, mostly reflecting variations in the ϕ profile, from 2×10^{-3} down to below 10^{-5} in amplitude.

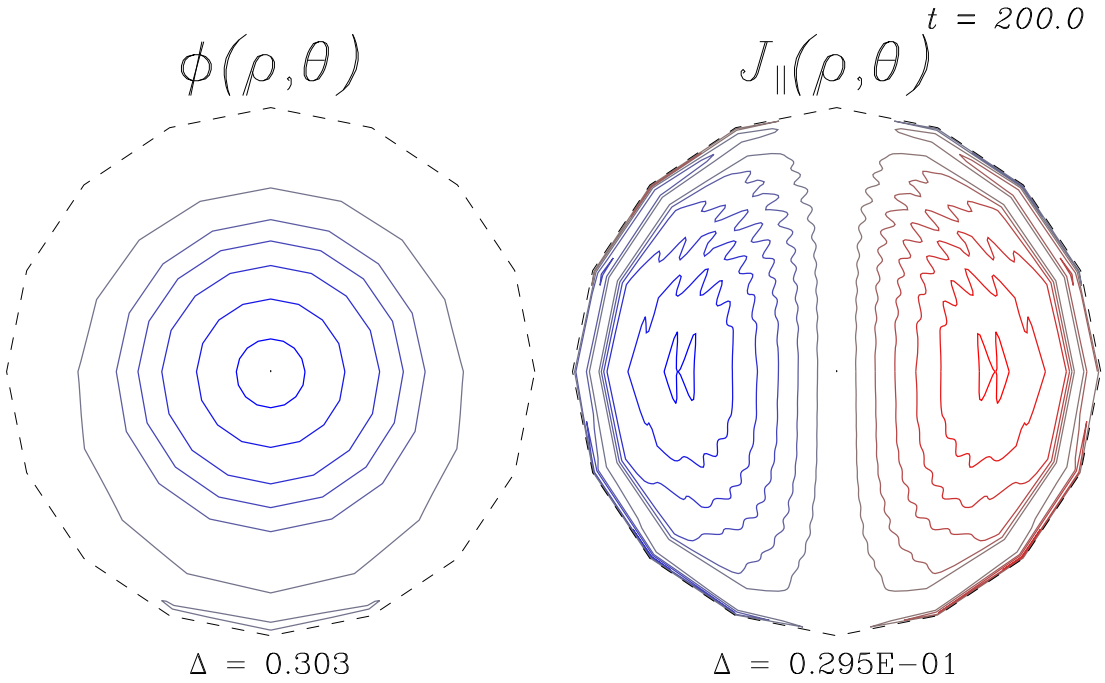

Fig. 10. Snapshot of the state at $t = 200a/c_s$ showing the electrostatic potential ϕ and the parallel current $J_{||}$. In each case red/blue are positive/negative and Δ gives the interval in normalised units. The basic force-balance equilibrium is reflected in the zonal component of ϕ (the part independent of θ) and the $\cos\theta$ sideband component of $J_{||}$ giving the Pfirsch-Schlüter current, in contrast to the structure in Fig. 5. The small Alfvén oscillation layers in $J_{||}$ and up/down shift in ϕ can still be seen, indicating that the force-balance equilibration is nearly but not totally complete.

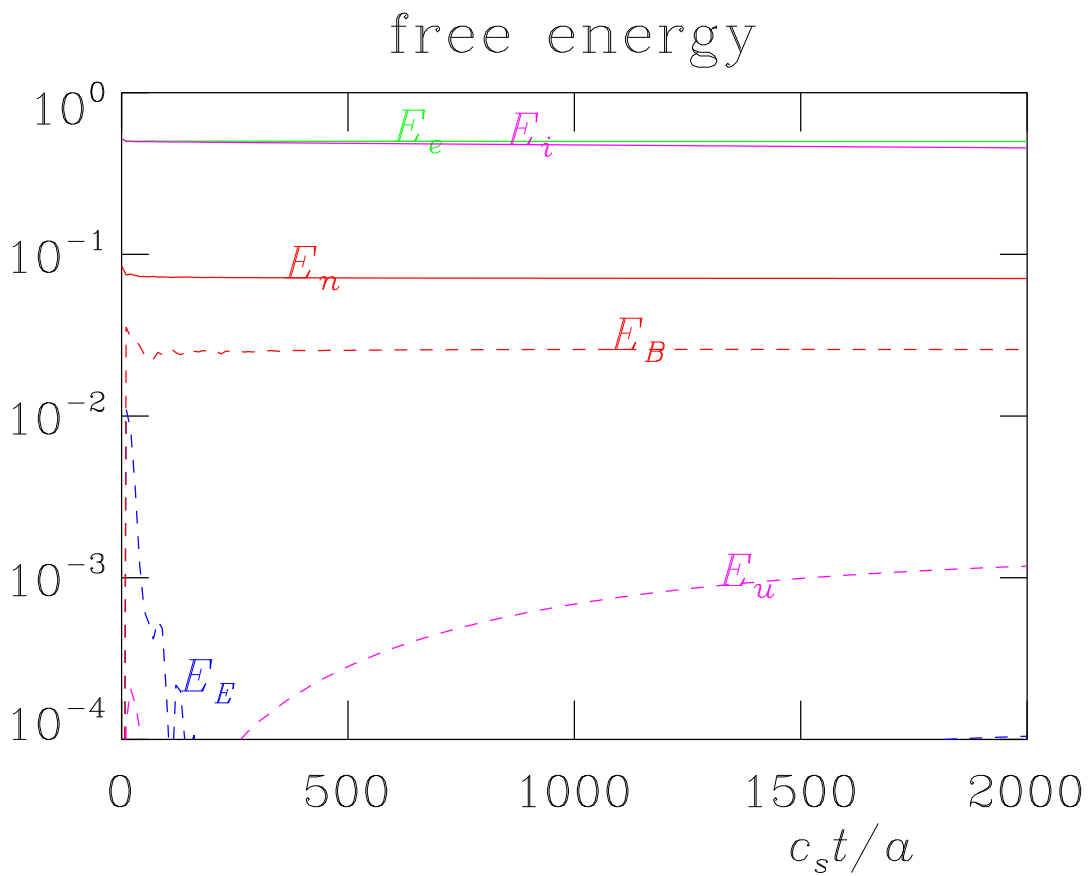

Fig. 11. Time traces of free energy components (due to ExB and diamagnetic ion flow 'E', density 'n', electron and ion temperature 'e,i', magnetic field and parallel electron flow 'B', and parallel ion flow 'u'). The electron and MHD energetics $E_{n,e,B}$ is nearly static. The ion thermal energy drops slightly, reflecting the slow neoclassical ion transport due to $\chi\nu_{NC}$. The perpendicular ion flow energy E_E is visible only for the initial equilibration phase but the parallel ion flow energy E_u rises slowly as the neoclassical flow relaxation begins to act.

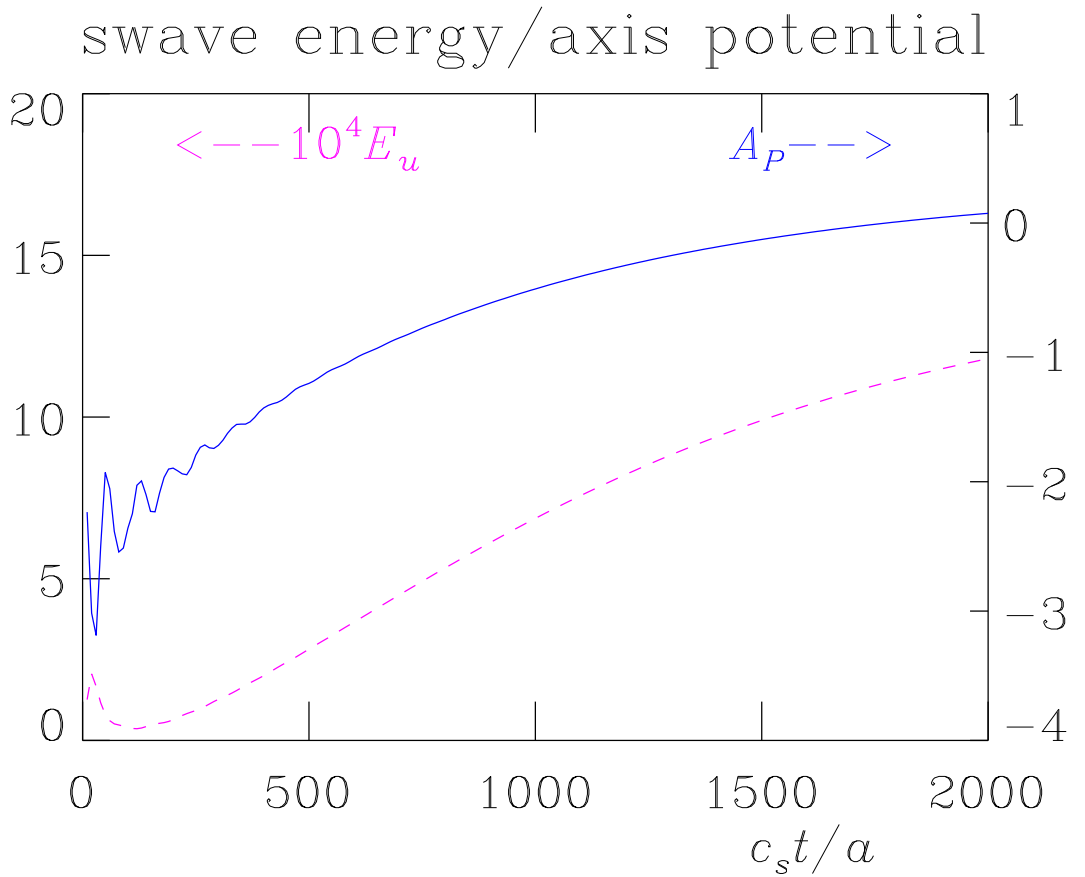

Fig. 12. Time trace of the axis value of ϕ (A_P) and the parallel ion flow energy (E_u). The acoustic oscillations from the initial equilbration phase become invisible after about $t > 500$. The slow rise of A_P shows relaxation away from the static force-balance level towards a value reflecting a finite overall perpendicular rotation. The evolution of E_u reflects the quasi-static ion flow divergence balance under collisional relaxation. The time scale of this is set by the neoclassical parallel ion viscosity coefficient ν_{NC}, and the level is set by the neoclassical thermal force coefficient α.

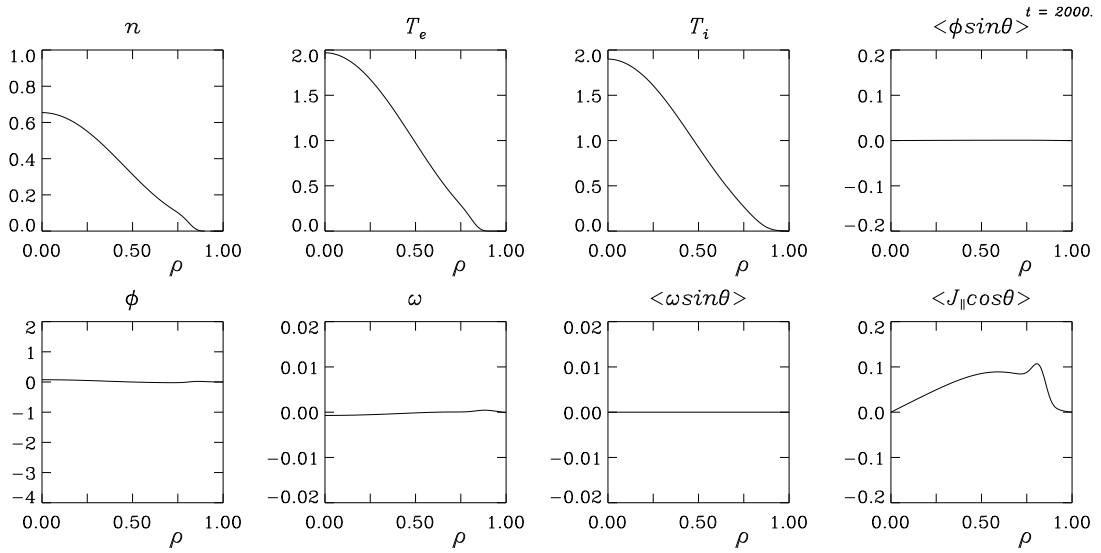

Fig. 13. Profiles (functions of ρ independent of θ) of the state at $t = 2000a/c_s$ showing zonal components of the density n, both temperatures $T_{e,i}$, the electrostatic potential ϕ and the vorticity ϖ, the $\sin\theta$ sidebands of ϕ and ϖ, and the $\cos\theta$ sideband of the parallel current $J_{||}$. Comparison to Fig. 8 shows that the Alfvén oscillation layers in the three sidebands damped away to small levels and the system is evolving quasi-statically under force-balance equilibration while the ion flow relaxes due to the neoclassical parallel ion viscosity. The small drop in T_i compared to T_e reflects the slow neoclassical ion transport due to $\chi\nu_{NC}$.

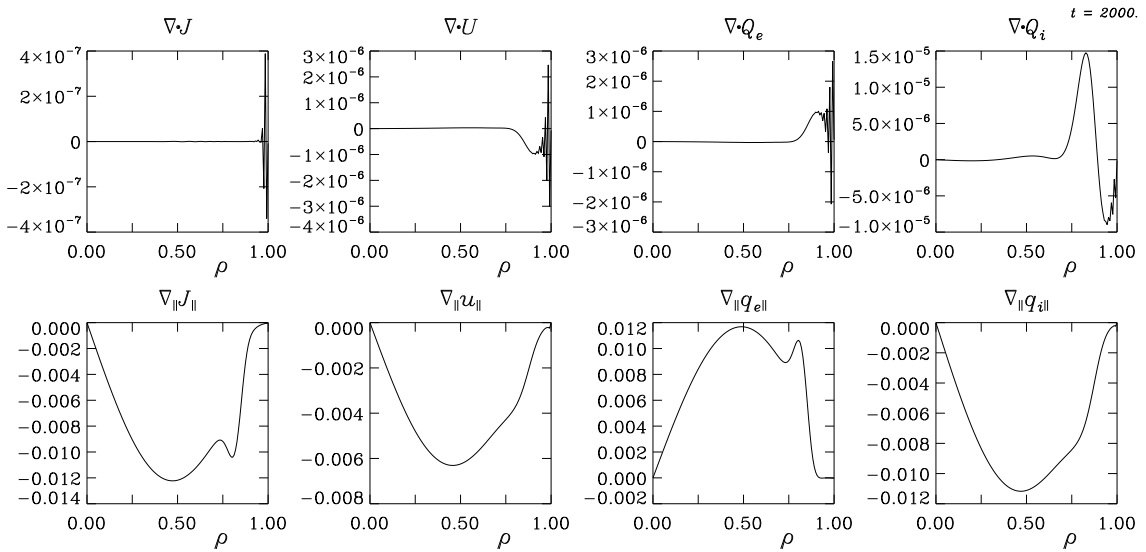

Fig. 14. Profiles (functions of ρ independent of θ) at $t = 2000a/c_s$ of the $\sin\theta$ component of the total gyrocenter divergences (that is, minus the polarisation component) in the current $\mathbf{J}$, ion flow $\mathbf{U}$, and electron and ion heat fluxes $\mathbf{Q}_{e,i}$, together with their corresponding parallel divergences $\nabla_\parallel$ on $J_\parallel$, $u_\parallel$, $q_{e\parallel}$, and $q_{i\parallel}$, respectively (note $\nabla_\parallel J_\parallel$ is actually $B\nabla_\parallel(J_\parallel/B)$, etc, but in this model $B = B_0$). In each case a total divergence consists of a geodesic curvature part acting on the zonal component of a state variable (plus the much smaller $l = 2$ sideband) and a parallel part acting on the $\cos\theta$ sideband of the coresponding flux variable, with the associated pairs being those given in Eqs. (70-73). The top row gives the total and the bottom row the parallel part. The ratio top/bottom row gives the closeness of equilibration. For $t = 2000$ all channels are in close balance, reflecting a well-relaxed equilibrated state. From here on, the system is a quasi-statically evolving equilbrium following collisional dissipation (profiles of ϕ, from neoclassical viscosity, and T_i, from neoclassical thermal transport).

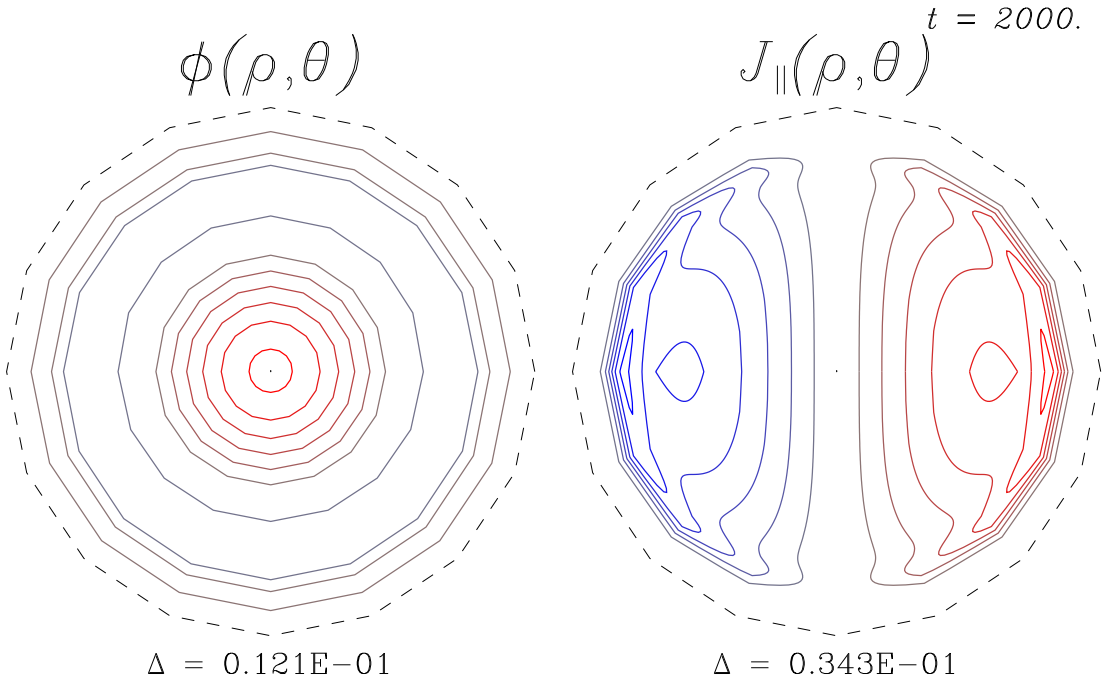

Fig. 15. Snapshot of the state at $t = 2000a/c_s$ showing the electrostatic potential ϕ and the parallel current $J_{\|}$. In each case red/blue are positive/negative and Δ gives the interval in normalised units. The small Alfvén oscillation signals visible in Fig. 10 are now absent. The edge layer in the Pfirsch-Schlüter current results from the inner transition boundary of the sink region at the outer edge. The potential structure is dominantly zonal, with the relaxing profile reflected in the changed interval and level (mostly positive at this time).

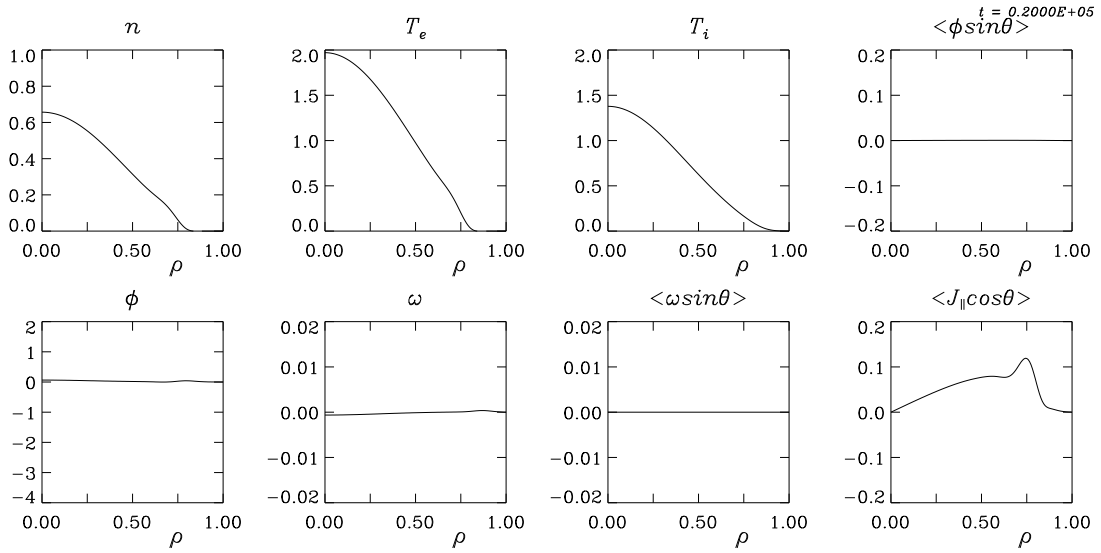

Fig. 16. Profiles (functions of ρ independent of θ) of the state at $t = 2 \times 10^4 a/c_s$ showing zonal components of the density n, both temperatures $T_{e,i}$, the electrostatic potential ϕ and the vorticity ϖ, the $\sin\theta$ sidebands of ϕ and ϖ, and the $\cos\theta$ sideband of the parallel current $J_{||}$. Comparison to Fig. 13 shows the same force-balance equilibration evolving quasi-statically under the neoclassical parallel ion viscosity and thermal conductivity. The decay of T_i and corresponding change to the profile of ϕ are visible.

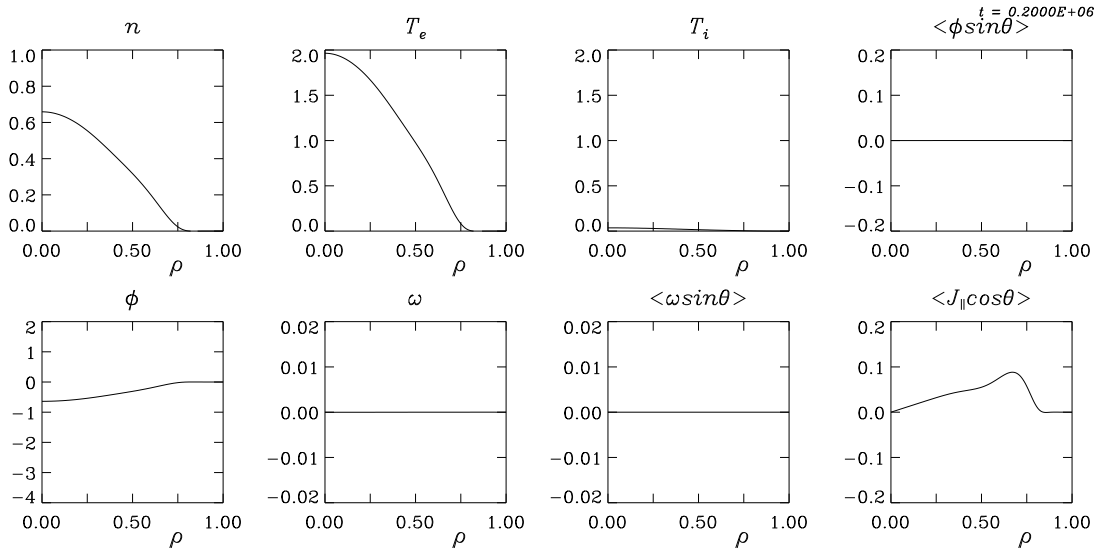

Fig. 17. Profiles (functions of ρ independent of θ) of the state at $t = 2 \times 10^5 a/c_s$ showing zonal components of the density n, both temperatures $T_{e,i}$, the electrostatic potential ϕ and the vorticity ϖ, the $\sin\theta$ sidebands of ϕ and ϖ, and the $\cos\theta$ sideband of the parallel current $J_{||}$. Comparison to Figs. 13,16 shows the same force-balance equilibration evolving quasi-statically under the neoclassical parallel ion viscosity and thermal conductivity. The decay of T_i and corresponding change to the profile of ϕ are now nearly complete.

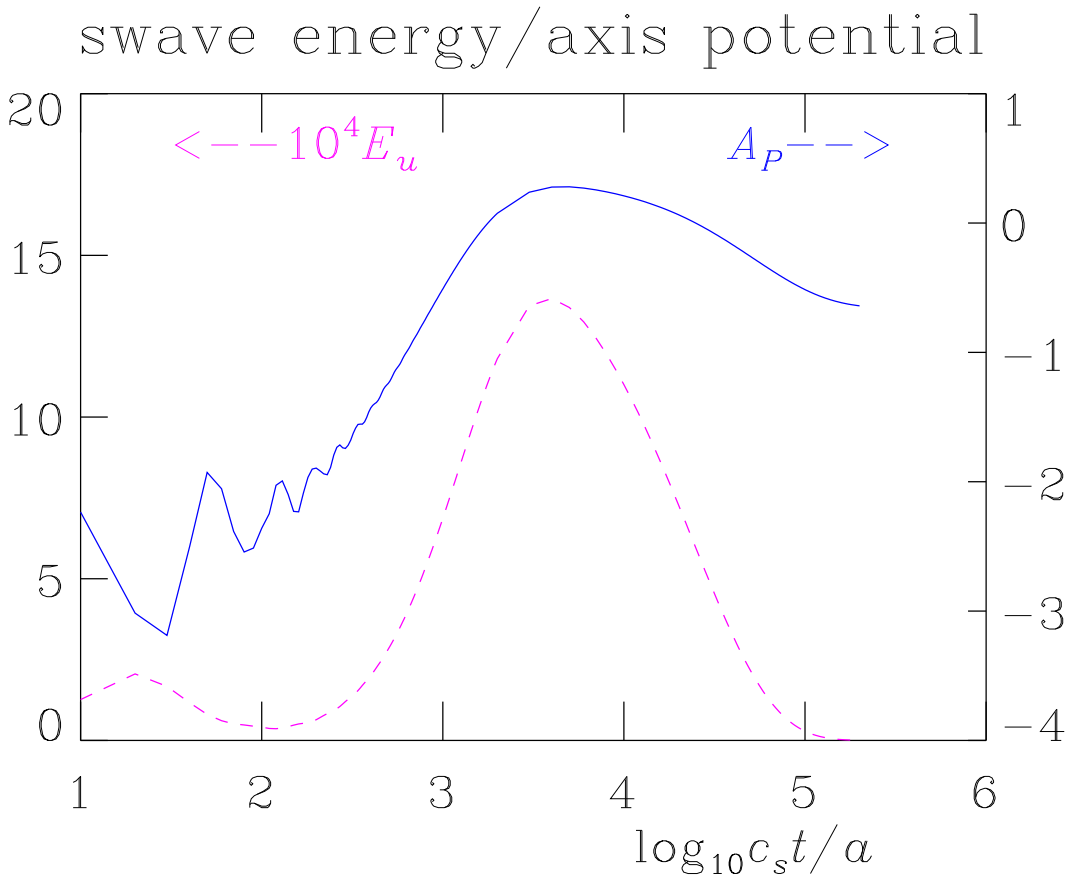

Fig. 18. Time trace of the axis value of ϕ (A_P) and the parallel ion flow energy (E_u), with the logarithmic time axis showing the various phases. The acoustic oscillations from the initial equilbration phase become invisible after about $t > 500$. The slow rise shows relaxation away from the static force-balance level towards a value reflecting a finite overall perpendicular rotation. The slow decay follows the neoclassical transport in the ion thermal conductivity channel. The evolution of E_u reflects the quasi-static ion flow divergence balance under collisional relaxation. As T_i decays the axis value of ϕ becomes negative again, eventually to balance $\tau_i \partial n/\partial \rho$, and E_u drops to zero.

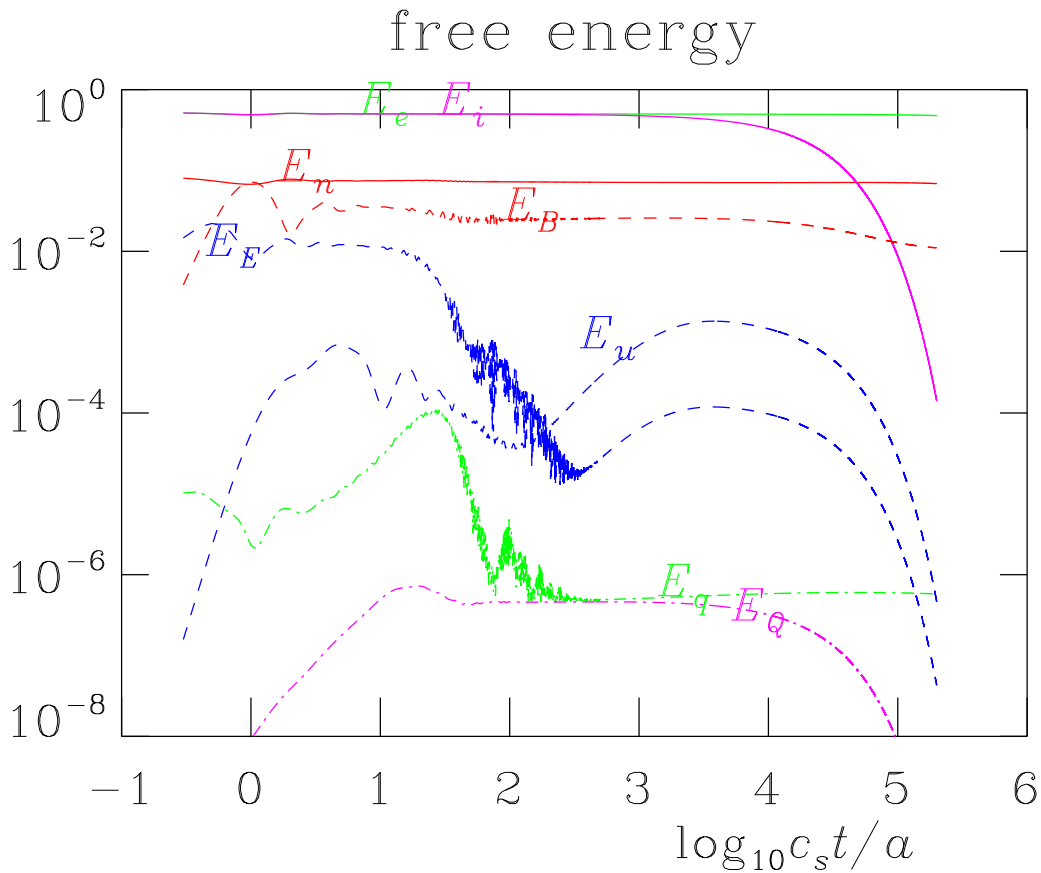

Fig. 19. Time traces of free energy components (due to perpendicular ion flow 'E', magnetic field/parallel electron flow 'B', thermal due to density 'n' and electron/ion temperature 'e,i', parallel ion flow 'u', and parallel electron/ion heat flux 'q,Q'), with the logarithmic time axis showing the various phases. At late times the heat fluxes follow the temperatures, the ion flow rises towards equilbration with the ion temperature gradient and afterward decays with it, and the drop in E_B following that in E_i is also visible. The dip in E_n during the Alfvén response phase reflects the involvement of the density profile in the energetics, but after $t = 10$ the electron density and temperature are negligibly damped over the entire run.

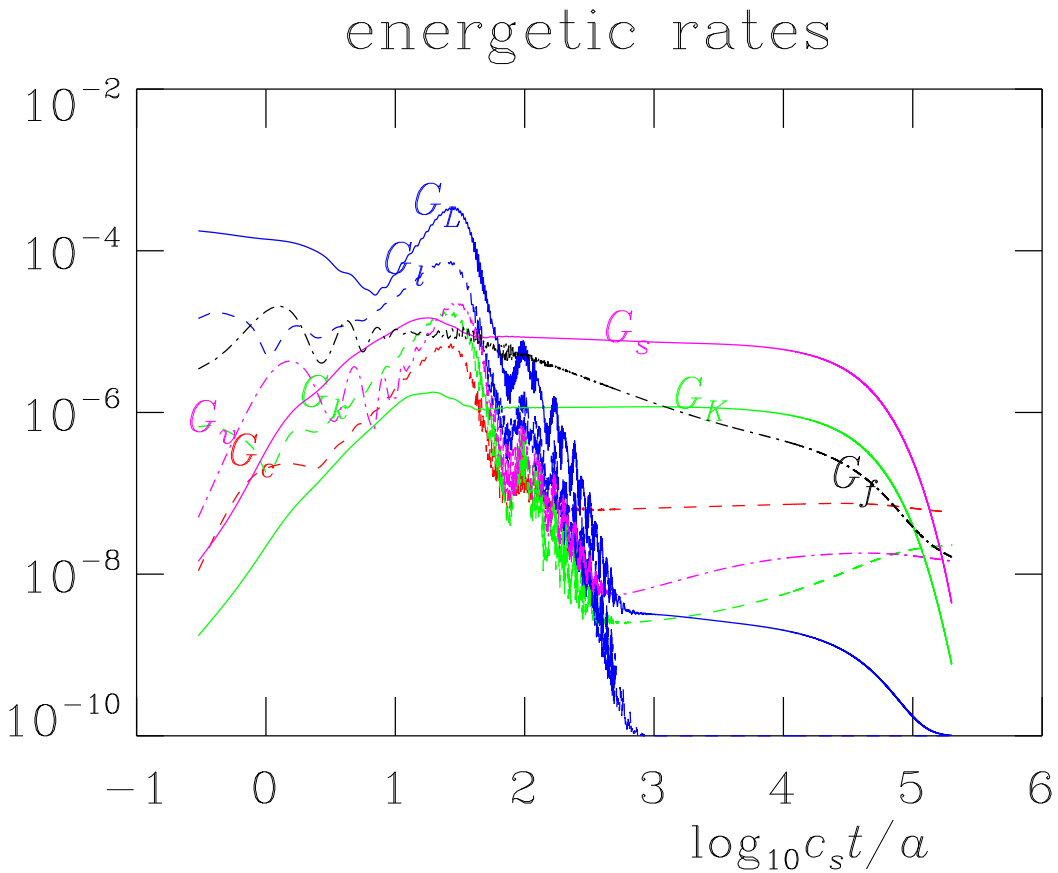

Fig. 20. Time traces of energetic dissipation components (due to electron and ion Landau damping 'l' and 'L', Braginskii resistivity and electron and ion thermal conduction 'c' and 'k' and 'K', neoclassical dissipation 's', and numerical dissipation due to hyper-diffusion 'v' and the edge layer sink 'f'), with the logarithmic time axis showing the various phases. The green dashed and solid lines are G_k and G_K respectively (with G_k the higher before about $t = 50$), and the higher of the blue lines is the ion one G_L. Most of the Alfvén continuum damping (peaking near $t = 20$) is in G_L, followed by G_l and then by G_v. Oscillations die away continually after about $t = 30$ and equilibration is increasingly solid

after $t = 100$, after which ion neoclassical thermal conduction is the dominant sink, with Braginskii ion thermal conduction a factor of about 6 behind. Over $1800 < t < 2000$ the total energetic decay rate is 9.38×10^{6} with an energetic error of 1.11×10^{-8}. Even G_c is 6.75×10^{8}, or about 6 times larger than the error.

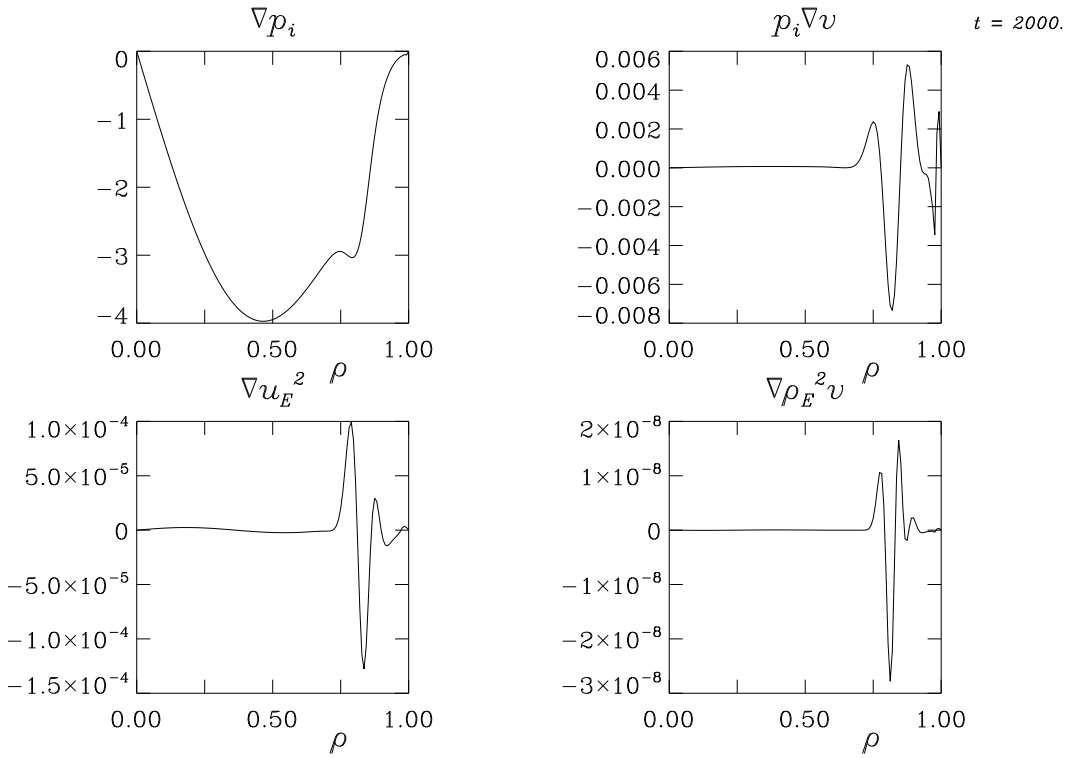

Fig. 21. Profiles (functions of ρ independent of θ) of the main ∇p_i term in the ion continuity equation against which ∇phi and $B\nabla_{\|}(u_{\|}/B)$ balance (upper left), the main FLR correction arising from $\rho_L^2 \nabla_\perp^2 \phi$ in the Hamiltonian H hence $p_i \nabla v$ (upper right), and the higher-order drifts corrections due to mu_E^2 and $\rho_E^2 \nabla_\perp^2 \phi$ in H hence ∇u_E^2 and $\nabla \rho_E^2 v$ (lower left and right, respectively) at $t = 2000$. The higher-order drifts corrections are much smaller than even the main FLR correction, with most of the signal near the edge sink layer hence even smaller in the core region. This indicates a negligible effect of the higher-order drifts on the result.

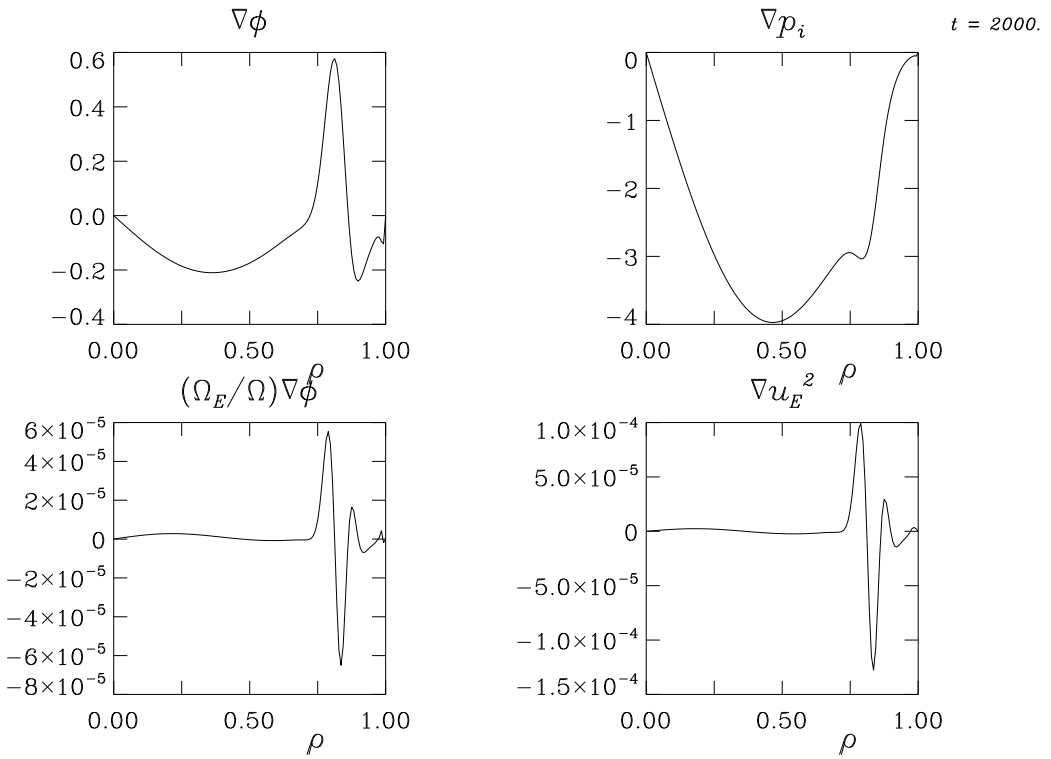

Fig. 22. Profiles (functions of ρ independent of θ) of the main ExB $\nabla_\perp\phi$ term in the drifts contribution to the total angular momentum (upper left), the main FLR correction arising from $\nabla_\perp p_i$, this time at unit order giving the diamagnetic flow term (upper right), and the higher-order drifts corrections due to ω_E^2/Ω times $\nabla_\perp\phi$ and $\nabla_\perp u_E^2$ (lower left and right, respectively) at $t = 2000$. The higher-order drifts corrections are much smaller than even the main FLR correction, with most of the signal near the edge sink layer hence even smaller in the core region. This indicates a negligible effect of the higher-order drifts on the result.

Bottom Line

- this shows a way to put neoclassical flow relaxation into a fluid model
  - by extension into a gyrofluid model
- the purpose is to demonstrate successive action of the processes at various time scales
- parameters satisfy $\omega_A \gg \omega_S \gg \omega_C \gg \omega_T$ without ordering the equations
- electron heat fluxes and current (MHD equilibrium) relax on ω_A
- then, flow and ion heat flux relax to force/divergence balance on ω_S
  - at this stage the "residual" flow depends on inital conditions
- then, the radial electric field relaxes on ω_C via collisions
  - this is equivalent to the collisional relaxation of the poloidal flow
    (and other neoclassical moments not included)
  - the flow evolves in quasistatic divergence balance
- finally, the zonal components of conserved quantities evolve via transport on ω_T
  - sources and sinks are only relevant on this time scale
  - all other quantities evolve quasistatically in neoclassical balance
- a gyrokinetic code can do this *iff*
  the collision operator and velocity-space resolution are good enough